

ON THE ORIGIN AND DISTRIBUTION OF C IV AND Si IV IONS
IN THE NEIGHBORING INTERSTELLAR MEDIUMLENNOX L. COWIE,¹ WILLIAM TAYLOR, AND DONALD G. YORK¹

Princeton University Observatory

Received 1980 December 22; accepted 1981 February 9

ABSTRACT

We present data on the C IV, Si IV, and N V absorption lines in 46 distant stars observed with the *IUE* spectrometer at FWHM resolution of 30 km s^{-1} . Sharp strong Si IV and C IV lines are regularly detected, while N V is not generally observed. Most of the Si IV and C IV lines probably arise in the H II regions surrounding the observed star or near neighbors. A simple analytic theory is given for these contributions, including the effects of ionization by a soft X-ray background. For some of the most distant field stars a photoionized contribution may be ruled out, but C IV absorption lines are detected. These particular lines are also unusual in that Si IV is not detected and that the lines are shallow and broad. We suggest that in these cases we are detecting contributions from the hot interstellar gas responsible for the O VI absorption lines. We obtain $\hat{n}(\text{C IV}) = 4 \times 10^{-9} \text{ cm}^{-3}$, consistent with the predictions of theories of the O VI absorption. An extended (radius $\gtrsim 100 \text{ pc}$) high velocity ($\sim 100 \text{ km s}^{-1}$) feature is observed in the Carina region.

Subject headings: interstellar: abundances — interstellar: matter — ultraviolet: spectra

I. INTRODUCTION

One of the major motivations for studying the interstellar medium (ISM) with ultraviolet spectrometers was the hope of detecting the C IV and Si IV ions predicted to be formed by the heating and ionizing mechanism maintaining the ISM (e.g., the review by Spitzer and Jenkins 1976). However, in the local ISM surveyed with *Copernicus*, absorption lines of these ions are weak or undetected (York 1974, 1977). This result is now understood in terms of the high charge-exchange rates of these species with neutral hydrogen (reviews by Dalgarno and Butler 1978; Watson 1978). It is paradoxical, therefore, that one of the most exciting results to emerge from the *IUE* satellite has been the widespread detection of Si IV and C IV absorption lines (Bruhweiler *et al.* 1979; Black *et al.* 1980; Smith, Willis, and Wilson 1980).

The existing data are fragmentary and in some cases are derived from programs covering special classes of stars (X-ray binaries, binaries, Wolf-Rayet stars). In addition, none of the programs has had a large enough sample of stars to be capable of supporting detailed interpretation on its own, while combining the observations is not straightforward owing to nonuniformity in the data reduction procedures (though see the recent review by Jenkins 1980). Thus it is not surprising that different observers have come to radically different conclusions on the origin of the lines. Bruhweiler *et al.* argue for a collisional ionization mechanism in 10^5 K gas while Black *et al.* conclude that the absorption arises from the H II regions around the hotter stars.

In the present paper we present data on interstellar Si IV, C IV, and N V absorption in 46 distant stars

observed with *IUE*. This sample was also obtained for a different purpose (*viz.*, studying the velocity distribution of gas in the neighboring interstellar medium), but is as well suited for studying the distribution of highly ionized atoms as is possible. However, the stellar sample is subject to the usual selection effects unavoidable in UV spectroscopy. The star must be of early spectral type and relatively unreddened. Many of these stars lie in associations and may correlate with highly disturbed regions such as supernova remnants or association shells similar to that in Orion (Cowie, Songaila, and York 1979). This must always be borne in mind in the interpretation of the data. The sample of stars and our data reduction procedure are discussed in § II.

In contrast to the nearby *Copernicus* observations, C IV is detected in almost all stars and Si IV in many. Positive N V detections are extremely rare. (We have no unambiguous cases, and eight dubious detections.) We attempt to relate the strength of the features to galactic morphology, to spectral temperature of the observed star, to length of the line of sight, and to intercepted objects along the line of sight (§ III). In this section we also consider the velocity structure of the absorbing gas. We conclude that most of the strongest Si IV and C IV absorption line features arise in H II regions either surrounding the observed stars or surrounding other very early type stars along the line of sight, and a simple analytic theory for the expected column density of the species including ionization by the soft X-ray and EUV background is given for both cases (§ IV). Weak broad C IV lines are seen in at least two of the most distant stars without corresponding Si IV absorption. In these cases we favor a general interstellar origin. The results may be interpreted in terms of the

¹ Guest observers on the *IUE* satellite, operated by NASA.

theory of evaporative interfaces (Cowie and McKee 1976; Cowie *et al.* 1979) and are consistent with the O VI absorption lines observed locally (§ V). Finally in one case (Carina) we see a high-velocity (-100 km s^{-1}) feature where C IV and Si IV most probably arise in a radiative shock (§ VI).

It is aesthetically unfortunate that several origins must be postulated for the Si IV and C IV lines and that no single theory seems capable of explaining the observations. However, as observations become more detailed, it may be unrealistic to expect simple interpretations.

II. OBSERVATIONS

The properties of the observed stars are given in Table 1. We list galactic longitude and latitude; spectral type; apparent visual magnitude; reddening; stellar radial velocity; distance based on spectral type, apparent magnitude, and extinction; distance based on association membership; whether the star is a known binary; the velocity with respect to the local standard of rest (LSR) due to galactic rotation expected at the observed star; and the exposure time of the observation. The position of the stars in the disk relative to the Sun is shown in Figure 1.

TABLE 1
PROPERTIES OF OBSERVED STARS

HD	l^{a}	b^{a}	MK ^a	V^{a}	E_{B-V}^{a}	V_{*}^{b} (km s^{-1})	$v \sin i$	d_1^{b} (kpc)	d_2^{a} (kpc)	Assoc. ^a	Binary ^c	V_{gr} (km s^{-1})	T_{exp} (min)
108	117.9	+1.2	O6:f	7.40	0.50	-55.1	114	1.9	2.51	Cas OB5	b	-21	100
2905	120.8	+0.1	B1 Ia	4.16	0.33	5.7	62	0.9	0.9(1.1)	Cas OB14	no	-10	7
5005	115.0	-5.6	O6.5 V	7.8	0.41	-17.5	106	1.88	Multiple	-20	83
40894	182.0	+2.8	B2 IV	7.6	0.16	1.06	no	0.9	40
42088	190.0	+0.5	O6.5 V	7.55	0.39	10.6	291	1.72	1.51	Gem OB1	no	6.4	47
46966	205.8	-0.5	O8 V	6.88	0.27	24.0	91	1.24	1.5	Mon OB2	no	11.2	15
47129	205.9	-0.3	O8p	6.08	0.36	1.0v	110	...	1.5	Mon OB2	b	13.3	14
47240	207.0	-0.8	B1 Ib	6.15	0.34	20.0	126	1.47	1.5	Mon OB2	no	13.5	50
47432	210.0	-2.0	O9.7 Ib	6.2	0.42	41.5	105	1.61	?	15.8	31
48099	206.2	+0.8	O7 V	6.38	0.27	15.1v	90	1.19	1.5	Mon OB2	b	11.0	11
53975	225.7	-2.3	O7.5 V	6.47	0.22	14.5v	412	1.32	1.32	CMa OB1	no	16.1	9
54662	224.2	-0.8	O6.5 V	6.21	0.35	41.8	95	0.98	1.32	CMa OB1	no	12.1	11
55879	224.7	+0.4	O9.5 II-III	6.00	0.12	14.6	31	1.69	1.32	CMa OB1	no	20.2	5
58350	242.6	-6.5	B5 Ia	2.41	0.02	23.8	57	0.74	no	8.0	25
75149	265.3	-1.7	B3 Ia	5.47	0.40	9.7	73	1.36	1.82	Vel OB1	no	5.5	75
91969	285.9	+0.1	B0 Ia	6.51	0.25	-12	96	2.47	2.51	Car OB1	no	-11.1	18
93843	288.3	-0.9	O5 III	7.34	0.34	-20.6	?	3.50	2.51	Car OB1	no	-9.0	24
96248	289.9	+0.3	B1 Iab	6.55	0.35	-37.9	92	2.19	2.0	Car OB2	no	-12.3	45
96670	290.2	+0.4	O8p	7.51	0.35	-8.9v	190	1.96	2.0	Car OB2	no	-11.9	70
96715	290.3	+0.3	O4 V	8.26	0.39	3.30	2.0	Car OB2	no	-13.7	129
96917	289.0	+3.0	O9.5 Ib	7.04	0.35	-1.8v	...	2.50	no	-11.8	67
101131	294.8	-1.6	O6 V	7.13	0.36	v	?	1.86	2.4	Crv OB1	b	-15.1	40
101205	294.8	-1.7	O7 III	6.48	0.39	-36.9v	...	1.52	2.4	Crv OB1	b	-12.9	18
101545A	294.9	-0.8	O9.5 Ib	6.38	0.30	-15.1	...	1.80	2.4	Crv OB1	b	-14.8	25
105056	298.0	-7.0	O9.5 Ia	7.55	0.33	-8.8	95	3.56	no	-25.2	43
135240	320.0	-2.6	O7.5(f)	5.1	0.26	6.4	?	0.96	b	-12.9	5
149038	339.4	+2.5	B0 Ia	4.89	0.32	9.5, 12, 5	133	1.06	1.38	Ara OB1a	no	-10.1	5
150041	336.2	-1.0	B0 Ib	7.06	0.32	-15.0	?	2.4	3.5	Ara OB1b	no	-29.5	47
150168	336.1	-2.2	B0.5I	5.64	0.20	8.8	154	1.8	1.38	Ara OB1a	no	-20.7	9
151804	343.6	+1.9	O8 Iaf	5.22	0.36	-55.3	124	1.69	1.91	Sco OB1	no	-14.1	8
152408	344.1	+1.5	O8 Iafpe	5.77	0.45	-132v	...	1.92	1.91	Sco OB1	no	-16.5	15
155985	343.6	-3.9	B0.5 II	6.47	0.46	-12.0	?	1.47	1.91	Sco OB1	no	-12.2	65
162978	5.0	+0.3	O7.5 II(f)	6.2	0.34	+0.5	...	1.64	no	4.6	13
164637	7.4	-0.2	B0.5 III	6.73	0.23	108	50	1.47	1.58	Sgr OB1	no	5.9	16
164794	6.0	-1.2	O4 V	5.97	0.35	20.7	168	1.21	1.58	Sgr OB1	no	3.8	8
167771	13.0	-1.2	O7 III(n)(f)	6.5	0.42	22.2	...	1.47	no	10.0	20
181858	29.0	-10.7	B3 V	6.7	0.17	1.1	67	0.38	no	4.3	35
184279	41.0	-6.2	B1 IV	6.8	0.29	7.7	141	1.01	13.6	50
186980	67.0	+3.1	O7.5 III(f)	7.5	0.39	22.7	138	2.43	no	+16.1	70
190918A	73.6	+2.1	O9.5 I+WR	6.80	0.41	-3.6	?	2.16	2.24	Cyg OB3	no	+9.8	50
191243	71.7	+1.0	B5 Ib	6.09	0.25	28.3	...	1.61	2.24	Cyg OB3	no	+9.3	110
191456	73.7	+2.1	B0.5 III	7.45	0.32	-2.0	80	1.81	2.24	Cyg OB3	no	+8.3	106
193322	78.0	+2.3	O9 V(n)	5.8	0.41	10.6	200	0.59	b	+2.6	16
195965	85.7	+5.0	B0 V	6.98	0.25	26.8	...	1.06	0.83	Cyg OB7	...	+0.4	23
203064	87.6	-3.9	O7.5 III	4.99	0.31	3.8v	328	0.86	0.83	Cyg OB7	no	-0.2	33
218915	108.1	-6.9	O9.5 Ia	7.18	0.29	-61.5	102	3.18	no	-30.2	40

^a For associations, radial velocity, V , l , b are all from Humphreys 1978. E_{B-V} is from her spectral type and $B-V$ (intrinsic) of Johnson 1966. Dist. 2 uses Humphreys (V , $B-V$) spectral type for all member stars.

^b Field star parameters from Humphreys 1970 or Humphreys 1975.

^c Association stars: from Humphreys 1978. Field stars from Kukarkin *et al.* 1969, Aitken 1932, and Innes 1927.

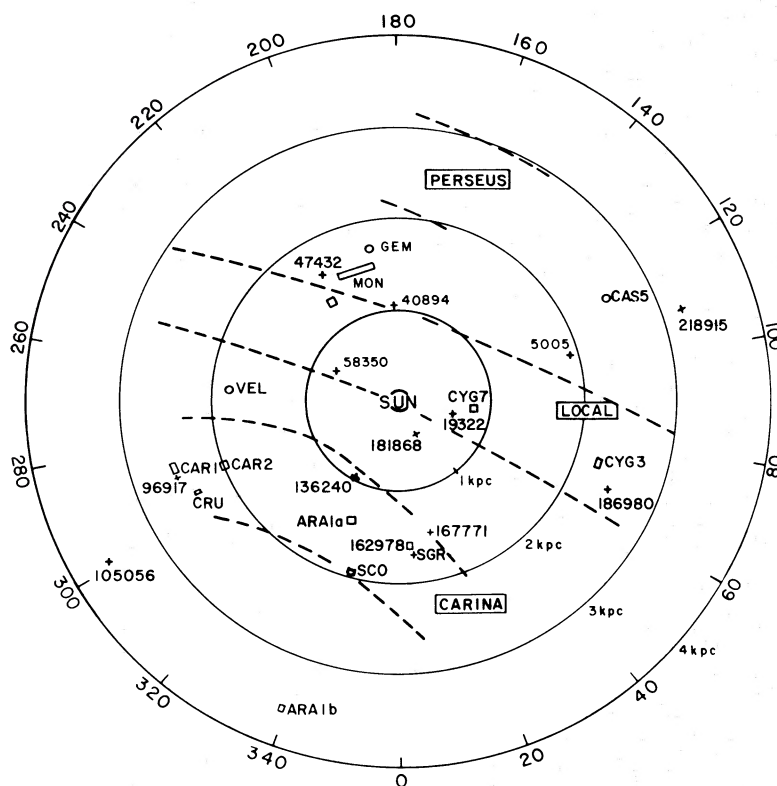


FIG. 1.—The positions of the stars observed with respect to the Sun. Where several stars in an association were observed, the region is shown as a block labeled by the association name. We have also schematically shown the local spiral arm structure according to Humphreys 1976. The arms are labeled in the square boxes.

All observations were made in the high dispersion mode of the short wavelength prime camera aboard the *IUE* satellite (Boggess *et al.* 1978*a, b*) and reduced with the standard *IUE* procedures. (It should be noted that none of the data was reduced with the erroneous intensity transfer used for earlier data collected with the satellite.) One exposure was obtained for each star. The resolving power $\Delta\lambda/\lambda$ is approximately 1.2×10^4 .

In all cases the wavelength regions near the Si IV and C IV lines are well exposed for the SEC vidicon detector implying signal to noise in the range 10–20, or minimum detectable equivalent widths in the range 20–40 mÅ. Conservatively, in all stars features larger than 50 mÅ will be detected, while in a few stars features as weak as 20 mÅ can be seen. However, the quality of the data is not uniform, and in some stars the minimum detectable equivalent width is larger.

In an effort to obtain as accurate velocities as possible and to minimize the effect of wavelength shifts due to changes in the physical properties of the spectrometer, wavelength calibrations were made throughout our shifts so that each stellar exposure was made within 4 hours of a wavelength calibration. The data were reduced with the appropriate wavelength calibration rather than the standard calibrations which were taken only at biweekly intervals during the period of our observations. Corre-

ctions for Earth and satellite orbital velocities were made and the data reduced into LSR velocity space. It is hard to make an exact determination of how accurate our velocity scale is. Comparison with existing *Copernicus* and optical observations on some of the observed stars suggest it is probably determined to better than 10 km s^{-1} .

One of the major problems in reducing the data is that of fitting a continuum (Fig. 2). Since the stellar rotation velocities were not available at the time of observation, a few of the stars have narrow stellar lines. For the C IV lines the continua are generally relatively unambiguous. For the Si IV lines, however, it is often hard to separate out interstellar features in the base of the stellar lines. This is also the reason why we have not measured the Al III line where the problems are generally worse. Where a reasonable continuum could be estimated, we have fitted a polynomial (usually linear or quadratic) continuum, normalized the intensity to this, and prepared plots in LSR velocity space. Sample profiles for four stars are shown in Figure 3, while copies for all stars are available on request. Equivalent widths for specified absorption lines are computed during the final reduction procedure as are central velocities $\langle v \rangle$ and velocity dispersions $\langle (v - \langle v \rangle)^2 \rangle^{1/2}$. The averaging in both cases is of the form $\langle x \rangle = \int (1-f)x dv / \int (1-f) dv$, where f is the normalized flux and integration is over the absorption feature.

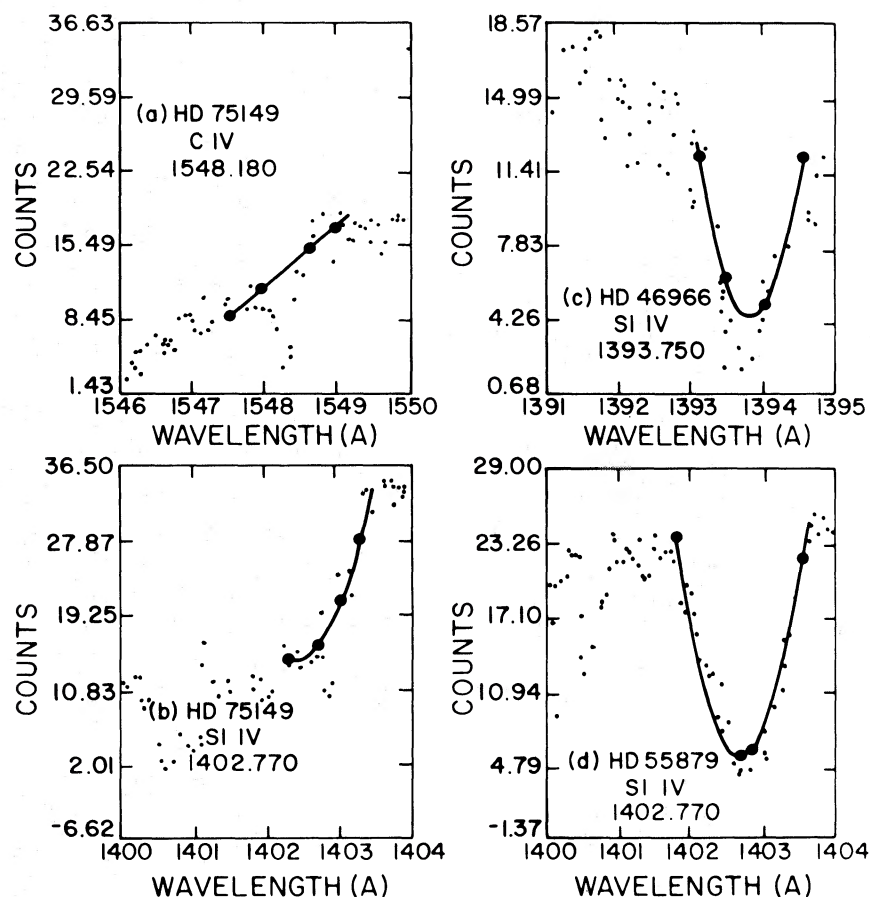


FIG. 2.—Sample profiles of the data in wavelength space. In Fig. 2a we show a C IV line with fitted continuum, and in Fig. 2b a well defined Si IV line. In Figs. 2c and 2d we have shown cases where the Si IV continuum is difficult to fit. In Fig. 2c a narrow line is unambiguously present but the equivalent width is poorly determined. In the case 2d there may exist a narrow Si IV line in the base of the stellar profile, but it cannot be unambiguously determined.

The equivalent widths of the lines are given in Table 2 for C IV, Si IV, and N V doublets. A general upper bound of 50 mÅ is assumed where the continuum was well determined and no absorption feature could be seen. Where problems with the continuum fit existed, a more generous bound has been estimated based on the maximum narrow line which could reasonably be placed in the base of the stellar line. For the measured equivalent widths, we have marked cases where we consider the continuum fitting more subjective, and where uncertainties in the equivalent widths are therefore large. For those cases where the equivalent width is well determined we also show the central velocity and velocity dispersion. For Carina where multiple components may be clearly seen, we have fitted the profile to distinguish the contributions. This anomalous region is not included in the subsequent general discussion but will be considered elsewhere (Cowie *et al.* 1981).

The data are not of sufficiently high quality to merit very detailed analysis. To make some crude allowance for saturation, however, we have translated those cases where equivalent widths are well determined into column densities using the doublet method. In each case we have

estimated limits on the doublet ratio based on a ± 25 mÅ uncertainty in the equivalent width of each member and quoted corresponding limits or lower bounds on the column density of the features (final columns of Table 2). This method is, of course, subject to well known problems when applied to the multiple saturated components expected in the ISM.

III. MORPHOLOGY

We have used the combined data sets of Tables 1 and 2 to investigate the properties of the C IV and Si IV lines and we present the results in graphical form in this section.

In Figure 4 we have plotted the column density of C IV and Si IV as a function of galactic longitude and of association membership. Two trends are suggested by this graph, though we do not consider either to be definitely established. The first is that column densities within associations tend to bunch in column density. The second, which is more speculative, is that there may be some tendency for those longitudes where lines of sight have the largest path through the arm regions (Fig. 1) to have the largest column densities.

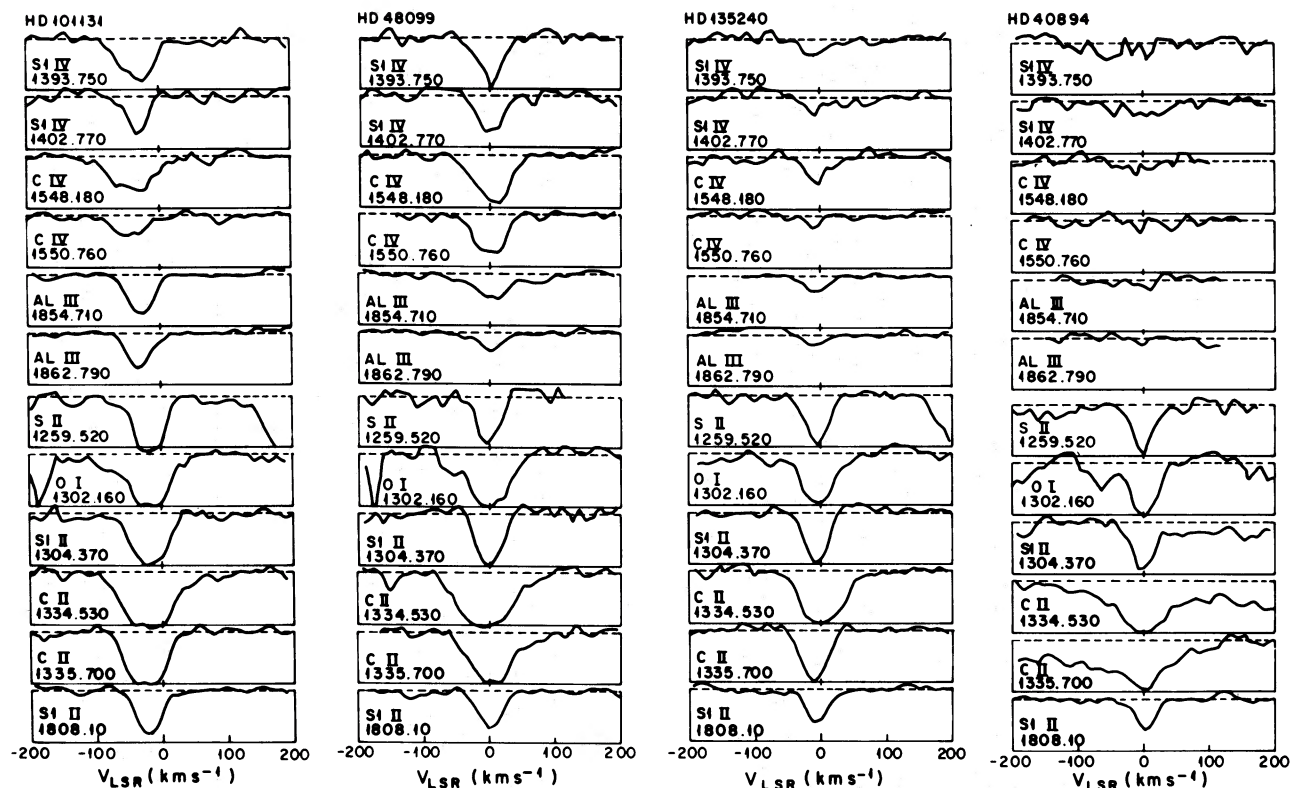


FIG. 3.—Some of the cases with well defined continua are shown in the normalized LSR velocity plots and compared with the profiles of lower ionization lines.

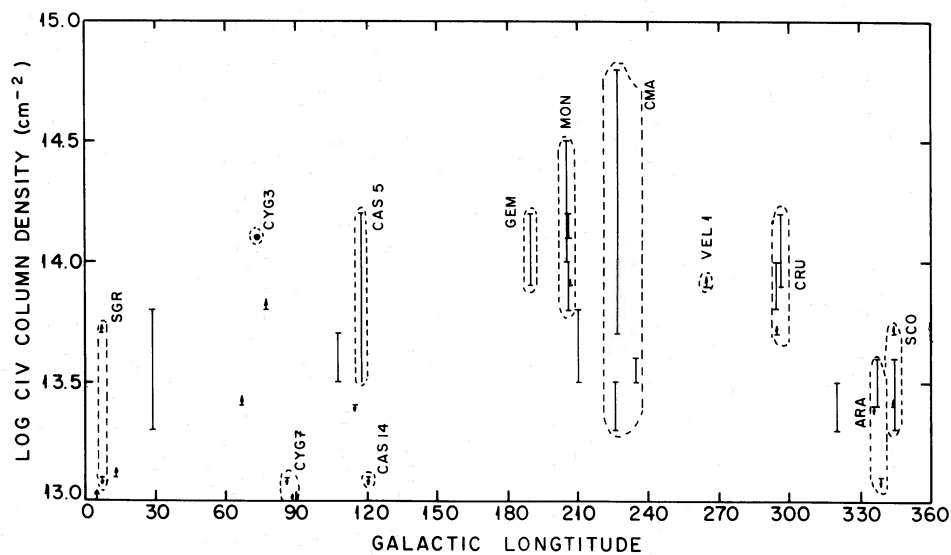


FIG. 4.—Column densities of C IV versus galactic longitude. Association membership is also indicated. Stars considered to be field members are labeled (F).

TABLE 2A
EQUIVALENT WIDTHS, VELOCITY STRUCTURE, AND COLUMN DENSITIES^a

HD	EQUIVALENT WIDTHS (mÅ)				LOG COLUMN DENSITIES			
	C IV	C IV	Si IV	Si IV	C IV	Si IV	Si IV	N V
108								
2905	134 (-26, 47)	≤70	<80	<70	13.5-14.2
5005	≤50	≤50	≤50	≤50	<13.1	<12.7	<13.4	<13.4
40894	<180	<50	<230	<160	<13.4	>13.8
42088	<270	<130	<260	<250	>13.4
46966	305 (-5, 43)	180 (10, 42)	220 (-2, 48)	170 ^b	13.9-14.2	>13.4	>13.4	>13.4
47129	390 (30, 39)	195 (35, 33)	140	190 ^b	14.0-14.1	>13.2	>13.2	>13.4
47240	270 (26, 29)	145 (12, 24)	180 (12, 32)	155 (11, 27)	13.8-14.1	>13.5	>13.4	>13.4
47432	230 (9, 48)	170 (8, 37)	180 (22, 28)	115 (24, 27)	>13.9	13.4-14.0	>13.7	>13.7
48099	120 (-26, 37)	<50	<50	<50	13.5-13.8	<12.7	<13.4	<13.4
53975	355 (6, 42)	240 (2, 33)	275 (1, 32)	200 (1, 33)	14.2-14.5	13.8-14.2	<13.4	<13.4
54662	80 (35, 19)	<50	<130	80 ^b	13.3-13.5	>13.2	>13.9	>13.9
55879	195 (9, 27)	125 (15, 32)	395 ^b	<235	13.8-14.8	>13.6	>13.4	>13.4
58350	195 (6, 24)	70 (2, 35)	<170	<130	13.5-13.6	<13.4
75149	150 (4, 50)	160 (8, 41)	130 (1, 25)	80 (-4, 21)	>13.4
101131	290 (-29, 38)	135 (-33, 30)	240 (-38, 34)	135 (-34, 23)	13.8-14.0	13.5-13.7	>13.4	>13.4
101205	300 (-20, 33)	180 (-28, 28)	135 (-34, 23)	140 (-32, 23)	13.9-14.2	>13.5	<13.4	<13.4
101545A	135 ^b	110 (-48, 15)	85 (-42, 29)	60 (-40, 14)	>13.7	>13.1	>13.4	>13.4
105056	250 ^b	95 ^b	100 (-25, 20)	60 (-36, 26)	...	>13.1	<13.4	<13.4
135240	125 (0, 27)	40 (-11, 16)	50 (-2, 14)	25 (-19, 11)	13.3-13.5	>12.8	<13.4	<13.4
149038	<50	<50	<50	<50	<13.1	<12.7	<13.4	<13.4
150041	95 (-2, 31)	<50	<50	70	13.4-13.6	>13.2	>13.4	>13.4
150168	<50	85 ^b	<145	<270	<13.4	...	>13.5	>13.5
151804	125 (-23, 39)	45 (-22, 26)	100 ^b (-22, 25)	15 (-41, 13)	13.3-13.6	13.2-13.5
152408	70	60 (-19, 19)	75 (-26, 33)	25 (-22, 20)	>13.4	>12.8
155985	190 (-10, 35)	<260	<100	<130	>13.7	...	<13.4	<13.4
162978	25 (-4, 18)	20 (-2, 20)	<300	45 (-4, 21)	>13.0	>13.0	<13.4	<13.4
164637	<50	<50	<50	<50	>13.1	>13.0	>13.4	>13.4
164794	165 (-3, 42)	100 (1, 32)	185 (2, 27)	115 (3, 23)	>13.7	13.4-14.2	<13.4	<13.4
167771	55 (12, 14)	<50	60 (20, 14)	60 (2, 24)	>13.1	>13.1	<13.4	<13.4
181858	108 (-1, 27)	43 (-6, 37)	13.3-13.8	...	<13.4	<13.4
184279					13.9	13.9
186980	70 (24, 24)	50 (15, 20)	90 (7, 24)	30 (-3, 21)	>13.4	12.8-13.6	<13.4	<13.4
190918A	665 (21, 56)	285 (6, 56)	290 (12, 63)	(1, 58)	14.1	>14.0	<13.4	<13.4
191243	<120	<90	<50	25 ^b	<12.7	<13.4
191456				405 ^b
193322	185 (-7, 40)	50	75 (6, 39)	75 ^b	>13.7	>12.9
195965	<50	<50	<50	<50	<13.1	<12.7	<13.4	<13.4
203064	75 (19, 23)	20 (6, 11)	150 (7, 18)	115 (-14, 28)	>13.0	>13.4	>13.4	>13.4
218915	150 (-6, 54)	65 (12, 39)	<50	<50	13.5-13.7	>12.7	<13.4	<13.4

^a Velocity centroids and dispersions in km s⁻¹ are shown in brackets for well determined lines.
^b Uncertain owing to continuum fit or noise problems.

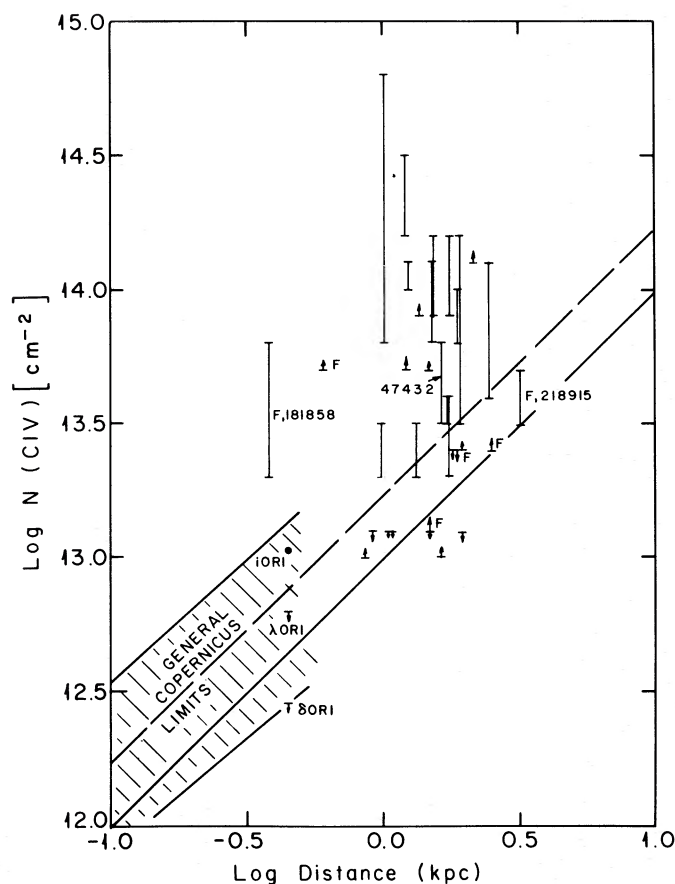


FIG. 5a

FIG. 5.—Column densities of C IV and Si IV versus distance of the observed star. Also shown are the predictions of a uniformly distributed hot interstellar medium. Published detections and upper limits from *Copernicus* on nearby stars are also shown, together with a schematic indication of the general upper limits from *Copernicus* collated by Jenkins 1980.

TABLE 2B
CARINA STARS

HD	V_{ter} (km s^{-1})	C IV	C IV	Si IV	Si IV
91969	-90	56	63	114	20
	-57	36	13	49	...
	-27	41	24	193	79
	1	77	14	69	24
93843	-104	50	...
	-55	165	80	175	105
	-18	95	45	60	35
96248	-90	...	210	160	100
	-52	160	95
	-34	...	180	220	110
96670-70 (noisy) ..	5	48	74	67	28
96670-150 (noisy)	150	120	80	80
96715	-95	177	124	72	37
	-55	79	50	59	45
	-20	113	86	43	28
96917	-86	180	110	80	75
	-40	80	45	40	90
	-5	125	55	60	35

NOTE.—No N V is observed in any of the Carina stars at above the 50 mÅ level.

In Figures 5a and 5b we plot C IV and Si IV column densities versus distance. It is useful in these plots to include the much more stringent limits obtained by *Copernicus* for nearby stars which emphasize that the more distant stars of the present survey do indeed show significantly higher column densities of C IV and Si IV. In Figure 5 we have also included lines showing the predictions of evaporative interface models and hot interstellar medium (HIM) models based on the discussion to be given in § V.

Two points should be made in considering Figure 5. A number of the stars observed in the present sample are very early, and this may produce a spurious impression of correlation of column density with distance, if the column density is larger for these stars. It is perhaps more significant to consider the scatter (more than an order of magnitude) in column density at a given distance. To account for this with a general interstellar mechanism would require that the absorption occur in a few large regions with typical separations of kiloparsecs. This brings us to the second point, which is that the results are consistent with but do not demonstrate (though see § V) the existence of a hot interstellar medium such as has been

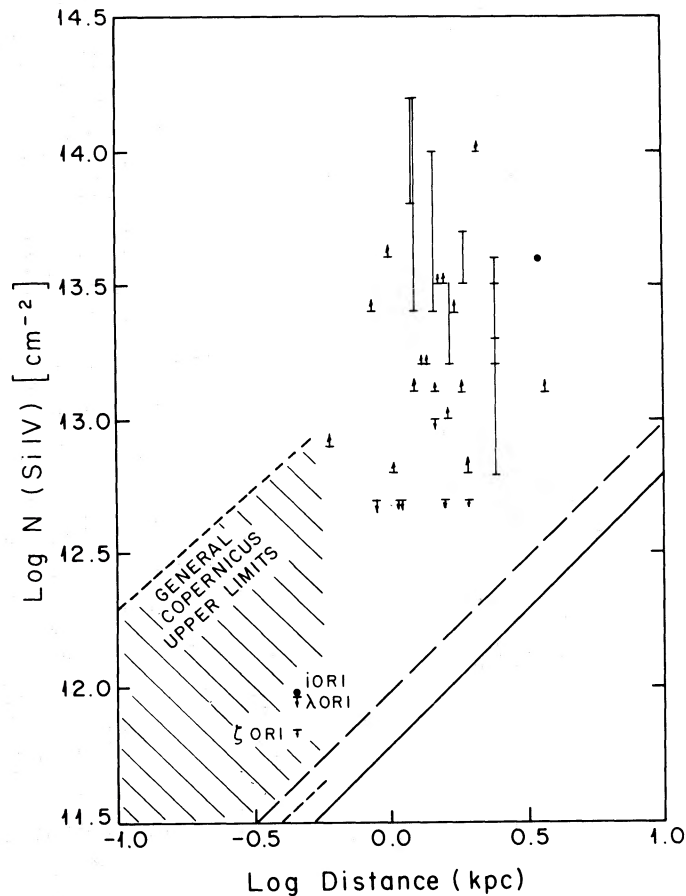


FIG. 5b

postulated to explain the O VI measurements. The detected Si IV column densities are above the theoretical predictions while the C IV detections lie above but close to HIM predictions. An important feature is that collisional ionization mechanisms predict much more C IV than Si IV whereas this is not generally true of the observed lines.

In Figures 6a and 6b we plot column densities versus spectral temperature of the observed star. We also show as solid lines the column density expected for a homogeneous H II region surrounding the star (Black *et al.* 1980, § IV). The predicted column density is of course an extremely sensitive function of spectral temperature but depends substantially less sensitively on density scaling as approximately $n_e^{1/2}$.

The first feature of Figure 6 to notice is that a number of stars of relatively low spectral temperature possess high column densities of C IV and Si IV. This point has been emphasized by Jenkins (1980) to argue against a general H II region interpretation. However, as he also recognized, many of the observed stars lie within rich associations containing substantial numbers of early type stars, and the probability of intercepting the H II region of

an earlier type star is not small. Case by case analysis given in § IV shows that many, though not all, of the anomalous stars fall in this category.

More positively, the data show some general consistency with the H II region theory in that stars with high spectral temperatures do show substantial amounts of C IV and Si IV. Some of the highest temperature stars in Figure 6 show less C IV and Si IV than would be predicted by the simple homogeneous theory, but this can be understood if the central regions of the H II region where C IV and Si IV form are evacuated by stellar winds or other mechanisms or if absorption of ionizing photons by dust grains within the H II region is important.

Finally in Figure 7 we present a plot of centroid velocity of observed features versus galactic rotation velocity at the star. Also shown are a number of simple theories for this quantity (1) $v_{\text{lsr}} = v_{\text{gr}}$ (stationary component at star), (2) $v_{\text{lsr}} = v_{\text{gr}} - 10 \text{ km s}^{-1}$ (expanding H II region at star), and (3) $v_{\text{lsr}} = \frac{1}{2}v_{\text{gr}}$ (uniform interstellar). Once again there are some anomalous cases which we will discuss individually, but the general trend corresponds somewhat to model (2) and the presence of galactic rotation may be clearly seen.

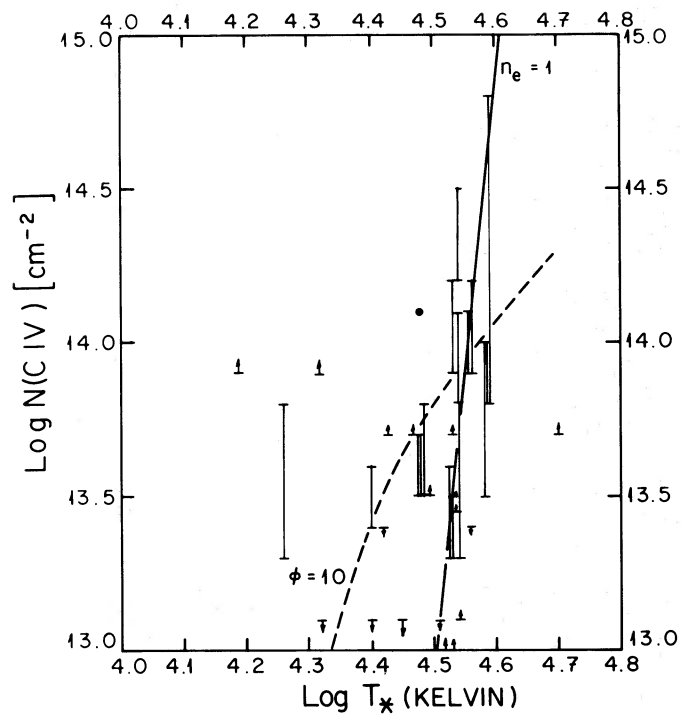


FIG. 6a

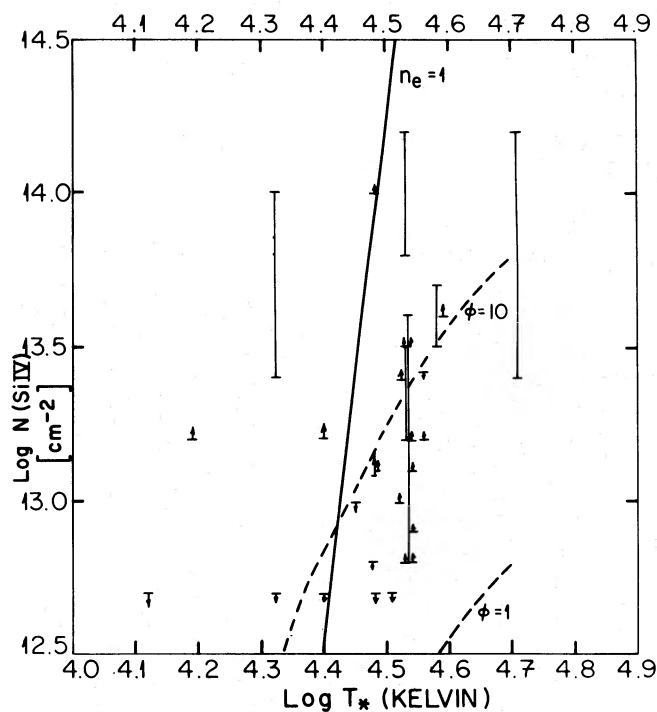


FIG. 6b

FIG. 6.—Column densities versus spectral temperature of observed star. Also shown are the predicted contribution of the H II region of the target star ($n_e = 1 \text{ cm}^{-3}$) as a solid line. When a uniform X-ray background is included, an additional contribution is obtained parametrized by the quantity ϕ (§ IV) and shown as a dashed line.

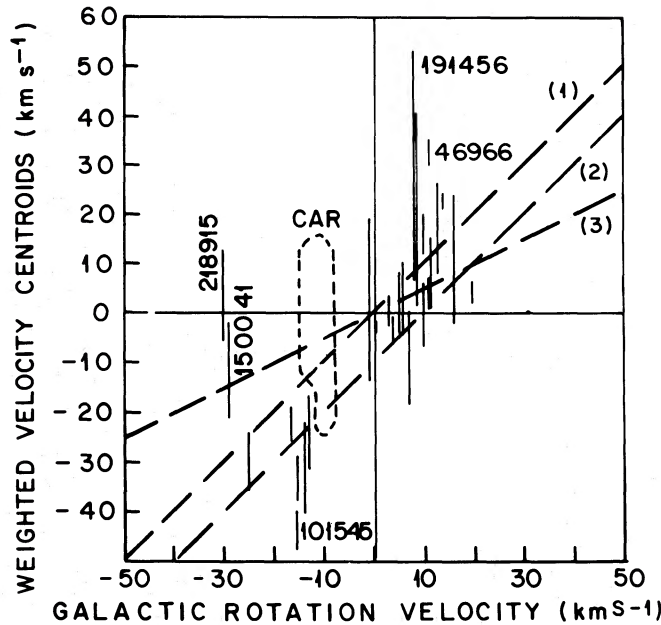


FIG. 7.—The range of centroid velocities of both C IV and Si IV absorption lines are shown as a function of the galactic rotation velocity at the star which would be observed from the Sun. The dashed line shows the position of the low velocity component observed in the Carina stars.

IV. CONTRIBUTIONS FROM H II REGIONS

a) Theory

For almost all stars (later than O5), C IV and Si IV form only in the centermost portion of the H II region where the photon flux is high. In these regions the opacity of both atoms and dust is small, and correspondingly the column densities of these species may be obtained in simple analytic form. This is particularly useful in calculating column densities of intercepted H II regions along the line of sight.

If the photoionization rate of ζ^i from ionization stage i to $i + 1$ is specified at a reference radius (R_n) for a given

spectral class of star (Table 3), we may write the ionization balance equation as

$$\alpha_{i+1} X_{i+1} n_e + \frac{\zeta^{i-1}}{y^2} X_{i-1} + C_{i+1} X_{i+1} n_H = \alpha_i X_i n_e + \frac{\zeta^i}{y^2} X_i + C_i X_i n_H, \quad (1)$$

where α_i is the recombination rate from level i to $i - 1$, C_i is the charge exchange rate of species X_i with neutral hydrogen and $y = r/R_n$. The dominant contribution to a given ion i comes at a point where the fraction in level

TABLE 3

H II REGION COLUMN DENSITIES ($n_e = 1 \text{ cm}^{-3}$)

T (K)	R_s (cm)	Adopted ^b R_a (cm)	C IV					Si IV				
			ζ^a (s ⁻¹)	ζn^c (s ⁻¹)	U^a	N_1 (cm ⁻²)	R_1 (cm)	ζ_a (s ⁻¹)	ζn^c (s ⁻¹)	U^a	N_1 (cm ⁻²)	R_1 (cm)
25,000	8(19)	1.4(12)	4.9(-9)	9.6(-21)	1.4(-12)	2.6(10)	5.0(13)	1.1(-2)	2.2(-14)	1.5(-6)	3.7(12)	7.2(16)
30,000	1.5(20)	1.4(12)	2.2(-4)	4.3(-16)	1.0(-8)	5.7(12)	1.1(16)	5.3	1.0(-11)	1.2(-4)	7.8(13)	1.5(18)
35,000	1.6(20)	7.0(11)	0.16	7.8(-14)	9.3(-6)	7.3(13)	1.4(17)	1.4(4)	6.9(-9)	6.4(-2)	2.0(15)	4.0(19)
40,000	2.0(20)	7.0(11)	8.5	4.2(-12)	3.7(-5)	5.7(14)	1.1(18)	2.6(5)	1.2(-7)	0.56	8.8(15)	1.7(20)
45,000	2.9(20)	1.05(12)	5.1(2)	5.6(-10)	1.5(-3)	6.2(15)	1.2(19)	8.7(5)	9.6(-7)	1.3	2.4(16)	4.7(20)
50,000	3.3(20)	1.05(12)	1.4(4)	1.5(-8)	3.0(-2)	3.2(16)	6.2(19)	1.7(6)	1.9(-6)	3.7	3.4(16)	6.6(20)

NOTES.—(1) Recombination rates: $\alpha_{\text{Si IV}} = 4.3 \times 10^{-12} \text{ cm}^3 \text{ s}^{-1}$, $\alpha_{\text{C IV}} = 3.8 \times 10^{-12} \text{ cm}^3 \text{ s}^{-1}$ evaluated at $T_e = 8000 \text{ K}$ from Aldrovandi and Péquignot 1973. (2) Abundances relative to hydrogen: $A_{\text{Si}} = 3.3 \times 10^{-5}$, $A_{\text{C}} = 3.3 \times 10^{-4}$. ζ is calculated from model atmospheres of Kurucz 1979 combined with carbon photoionization cross sections tabulated by Raymond 1976. Charge exchange rates $C_{\text{Si IV}} \sim 10^{-9} \text{ cm}^3 \text{ s}^{-1}$, $C_{\text{C IV}} = 1.6 \times 10^{-9} \text{ cm}^3 \text{ s}^{-1}$.

^a Definitions: $U = \alpha_{\text{H}} C_{\text{H}} \zeta_{i-1} / \alpha_i^2 \zeta_{\text{H}}$, $N_1 = \frac{1}{2} \pi A_x R_n \{ \zeta_{i-1} / \alpha_i \}^{1/2}$, $R_1 = \{ \zeta_{i-1} / \alpha_i \}^{1/2} R_n$.

^b Intermediate value for stars of this T_* from the tabulation of Snow and Morton 1976.

^c Normalized at $R_n = 10^{18} \text{ cm}$.

$i + 1$ is small and where $X_i + X_{i-1} = 1$ so that equation (1) may be simplified to read

$$\alpha_i X_i n_e + C_i X_i n_H = \frac{\zeta^{i-1}}{y^2} (1 - X_i); \quad (2)$$

or since

$$n_H = \frac{\alpha_H}{\zeta_H} n_e^2 y^2, \quad (3)$$

$$X_i = \frac{\zeta^{i-1}}{n_e y^2} \left(\alpha_i + y^2 \frac{\alpha_H C_i n_e}{\zeta_H} + \frac{\zeta^{i-1}}{n_e y^2} \right)^{-1}.$$

If the charge exchange term may be neglected

$$X_i = \left(1 + \frac{\alpha_i n_e y^2}{\zeta^{i-1}} \right)^{-1}; \quad (4)$$

and if the abundance of the atom is A_x by number, the integrated column density is

$$N(X_i) = n_e A_x R_n \int_{R_{\min}/R_n}^{\infty} \frac{dy}{(1 + \alpha_i n_e y^2 / \zeta^{i-1})}$$

$$= \left(\frac{\zeta^{i-1}}{\alpha_i} \right)^{1/2} n_e^{1/2} A_x R_n$$

$$\times \left\{ \frac{\pi}{2} - \tan^{-1} \left[\left(\frac{\alpha_i n_e}{\zeta^{i-1}} \right)^{1/2} \frac{R_{\min}}{R_n} \right] \right\}, \quad (5)$$

where we have assumed that the H II region is empty inside R_{\min} and homogeneous with electron density n_e outside this point. For R_{\min} small the dominant contribution to equation (5) arises at

$$r = \left(\frac{\zeta^{i-1}}{\alpha_i n_e} \right)^{1/2} R_n \equiv \frac{R_1}{n_e^{1/2}}$$

(Table 3). To justify the neglect of charge exchange, we require $U \equiv \alpha_H C_i \zeta^{i-1} / \alpha_i^2 \zeta_H \ll 1$. This equation is generally satisfied for the C IV and holds for Si IV when the temperature of the central star is less than or equal to 40,000 K.

We may also evaluate the column density at projected radius p through an intercepted H II region as

$$N(X_i) = \pi \left(\frac{\zeta^{i-1} n_e}{\alpha_i} \right)^{1/2} A_x R_n$$

$$\times \left\{ 1 - \frac{2}{\pi} \tan^{-1} \left[\frac{\alpha_i n_e (R_{\min}^2 + p^2)}{\zeta_{i-1} R_n^2} \right]^{1/2} \right\}. \quad (6)$$

The quantities $N_1 = \frac{1}{2} \pi A_x R_n (\zeta^{i-1} / \alpha_i)^{1/2}$ and

$$R_1 = (\zeta^{i-1} / \alpha_i)^{1/2} R_n$$

are given in are given in Table 3 for the species of interest. The first gives the column density through a homogeneous H II region of density $n_e = 1 \text{ cm}^{-3}$. The second gives the characteristic radius at which the dominant contribution to the ion arises. This simple theory reproduces well the numerical results of Black *et al.* for target stars, $T_* \leq 40,000 \text{ K}$. However, it should be noted that for $T_* > 40,000 \text{ K}$ in the case of Si IV the column density is

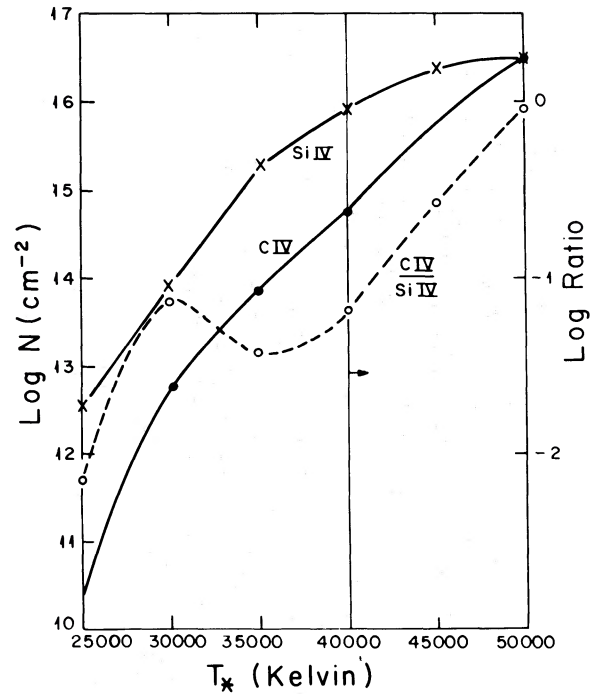


FIG. 8.—Column densities of Si IV, C IV, and their ratio as a function of T_* . To the right of the marked line the C IV/Si IV ratio may be underestimated as discussed in the text.

overestimated by factors of several owing to the neglect of charge exchange (low n_e) or hydrogen opacity (large n_e).

We may summarize the results as follows (Fig. 8). In order to obtain an observable amount of Si IV or C IV ($\geq 10^{13} \text{ cm}^{-2}$) the spectral temperature of the star responsible must exceed about 30,000 K and 35,000 K, respectively. The column density scales as $n_e^{1/2}$, and the ratio of C IV to Si IV is dependent only on T_* . The ratio of Si IV to C IV is shown as a function of spectral temperature in Figure 8. The value is generally around 10 for the spectral classes of interest. For the hottest stars, C IV column densities will exceed Si IV densities.²

For projected radii larger than the dominant radius the observed column density relates to the column density that would be seen if the stars were the target as $R_1 N_1 / p$. The projected radius at which observable amounts of C IV and Si IV will be present is a very sensitive function of spectral type owing to the R_1^2 dependence. Typically we require $p \leq 25 \text{ pc}$ (40,000 K) and $p \leq 0.4 \text{ pc}$ (35,000 K) to obtain C IV column densities in excess of 10^{13} cm^{-2} . For hotter stars, observable quantities of C IV may be seen throughout the Strömgren sphere.

We have neglected two additional processes in the above discussion. The first is absorption of C IV and Si IV ionizing photons by dust grains within the H II region (Sarazin 1976). At the photon energies of interest

² This applies only if the central region of the H II region is filled. If the central regions are evacuated the C IV/Si IV ratio will be reduced. The C IV/Si IV ratio is also reduced in the case of intercepted regions.

($\sim 30\text{--}50$ eV) the grains reach optical depth unity at a radius $\sim 30\text{--}300$ pc/ n_e . Beyond this distance the ionization rate drops off rapidly. It is possible, therefore, that the earliest type stars may be dust opacity bounded, which would reduce the Si IV column densities. C IV column densities are less likely to be affected since they form at smaller radii.

Second, we have neglected ionization by a soft X-ray or cosmic ray background or by soft X-rays from the star itself. Since the dominant effect is Auger ionization, this may produce traces of C IV and Si IV throughout the H II region even for low T_* stars. The dominant contribution again arises in the interior where charge exchange with neutral hydrogen may be neglected. Thus we may again neglect radiative transfer.

We have evaluated the Auger ionization rate ζ^{i-1} from cross sections tabulated by Weisheit (1974) and Daltabuit and Cox (1972) together with an assumed soft X-ray flux of $1.50 \times 10^4 \phi$ photons $\text{cm}^{-2} \text{s}^{-1} \text{keV}^{-1}$ at the Si II $2p$ threshold energy of 125 eV and 2000ϕ photons $\text{cm}^{-2} \text{s}^{-1} \text{keV}^{-1}$ at the C II threshold energy of 296 eV. The quantity ϕ is a scale factor allowing for the expected large variations in the X-ray flux from region to region. The results are given as subscripts to Table 4. Throughout the H II region we expect C II and Si II to be the dominant ionization stage whence

$$\alpha_{i+2} n_e n(X_{i+2}) + C_{i+2} n_H n(X_{i+2}) = \zeta^{ai} n(X_i)$$

or

$$n(X_{i+2}) = \frac{\zeta^{ai} n_e A_x}{\alpha_{i+2} n_e + C_{i+2} \alpha_H n_e^2 y^2 / \zeta_H}$$

Hence

$$\begin{aligned} N(X_{i+2}) &= \frac{\zeta^{ai} A_x R_n}{\alpha_{i+2}} \int_0^\infty dy \left(1 + \frac{C_{i+2} \alpha_H n_e}{\zeta_H \alpha_{i+2}} y^2 \right)^{-1} \\ &= \frac{\pi \zeta^{ai} A_x R_n}{2 \alpha_{i+2}} \left(\frac{\zeta^H \alpha_{i+2}}{C_{i+2} \alpha_H n_e} \right)^{1/2} \end{aligned}$$

The column density due to this effect scales as $n_e^{-1/2}$, ϕ , and $\zeta_H^{1/2}$. Relevant quantities may be found in Table 4.

We have plotted the contribution from this effect as a dashed line in Figure 6. It is only significant if ϕ is larger

than the local value. However, this may easily be the case if many of these stars are near fossil supernova remnants or other active regions.

V. HOT IONIZED MEDIUM

a) Theory

The local O VI absorption lines observed by *Copernicus* are now believed to originate either directly in a uniformly distributed hot intercloud medium or in the evaporating surface of clouds within such a hot gas. The average local density in the disk is $n(\text{O VI}) \approx 2 \times 10^{-8} \text{cm}^{-3}$. Depending on the model chosen, the expected column densities of C IV, Si IV, and N V may be evaluated and are proportional to $n(\text{O VI}) \cdot d$ if we assume that the region observed by *Copernicus* ($d \lesssim 1$ kpc) is representative. For evaporative interfaces the ratios may be obtained from the time dependent ionization calculations of Weaver *et al.* (1977) as Si IV/O VI = 0.01, C IV/O VI = 0.16, N V/O VI = 0.06. Similar ratios are obtained for a time-dependent cooling gas (Jenkins 1980).

We therefore take

$$N(\text{Si IV}) = 6 \times 10^{11} \left[\frac{n(\text{O VI})}{2 \times 10^{-8}} \right] d(\text{kpc}) \text{cm}^{-2},$$

$$N(\text{C IV}) = 9.6 \times 10^{12} \left[\frac{n(\text{O VI})}{2 \times 10^{-8}} \right] d(\text{kpc}) \text{cm}^{-2},$$

$$N(\text{N V}) = 4 \times 10^{12} \left[\frac{n(\text{O VI})}{2 \times 10^{-8}} \right] d(\text{kpc}) \text{cm}^{-2}.$$

These results are compared with the observations in Figure 5.

These models predict that HIM Si IV and N V should *not* be detected by *IUE* at our present sensitivity but that in the more distant stars C IV may be detectable if it is not dominant by a photoionized component.

b) Comparison with Observation

In Table 5 we give a list of those stars whose column density of C IV or Si IV is high compared to the values for an H II region with $n_e = 1$, $\phi = 1$. We also show the

TABLE 4
X-RAY IONIZED H II REGIONS

T_* (K)	R_* (cm)	ζ_H (at R_*) ^a (s^{-1})	$N(\text{C IV})[\phi = 1]$ ^a (cm^{-2})	$N(\text{Si IV})[\phi = 1]$ (cm^{-2})
25,000	1.4(12)	7.9(4) ^b	2.3(12)	6.9(11)
30,000	1.4(12)	4.8(5) ^b	5.6(12)	1.7(12)
35,000	7(11)	2.4(6) ^b	6.4(12)	1.9(12)
40,000	7(11)	5.0(6) ^b	9.6(12)	2.8(12)
45,000	1.05(12)	7.1(6) ^c	1.7(13)	5.1(12)
50,000	1.05(12)	1.0(7) ^c	2.0(13)	6.0(12)

NOTE.—For charge exchange rates, recombination coefficients, and abundances, see Table 3.

^a Calculated for C II K shell ionization rate = $4 \times 10^{-16} \text{s}^{-1}$. Si II L shell ionization rate = 10^{-14}s^{-1} .

^b Black *et al.* 1980.

^c From stellar atmosphere tabulation of Kurucz 1979.

TABLE 5
 HIGH COLUMN DENSITY STARS

HD	Log T_* (K)	Log $N(\text{C IV})$ (cm^{-2})	Log $N(\text{Si IV})$ (cm^{-2})	Intercepted Star and Projected Distance	Required ϕ	Required n_e (cm^{-3})
47240	4.32	> 13.9	13.4–14.0	O4 V, 35 pc		
47432	4.48	13.5–13.8	< 12.7	O4 V, 100 pc	6	36
55879	4.48	13.5–13.6	...		6	36
75149	4.19	> 13.9	> 13.2	O4 I,(n)f, 100 pc		
101545	4.48	> 13.7	> 13.1	O6, 20 pc	9	81
150041	4.40	13.4–13.6	> 13.2	O5 II, 12 pc	11	...
155985	4.43	> 13.7	11	...
181858	4.26	13.3–13.8
190918	4.48	14.1	> 14.0	O6.5, 4 pc	22	500
218915	4.48	13.5–13.7	< 12.7	...	6	36

required n_e or ϕ (for $n_e = 1 \text{ cm}^{-3}$) required in those cases where the column density could plausibly arise in a circumstellar H II region.

We have searched for the nearest neighboring early type star in each case. Where a plausible candidate exists, this is listed together with the projected distance from the line of sight to the target star. We consider that a photoionization mechanism augmented by a soft X-ray ionizing flux can account for the observed column densities in almost all stars. We do not think such a mechanism can account for the stars 47432 and 218915. In these two

cases we base this judgement on the Si IV/C IV ratio which is anomalously low (C IV is detected but Si IV is not); however, it is possible that an X-ray ionized H II region could possess such a low ratio. Both stars are distant and lie near the predicted C IV versus distance relationship. Consideration of the velocity structure of these lines shows that they are unusually broad and

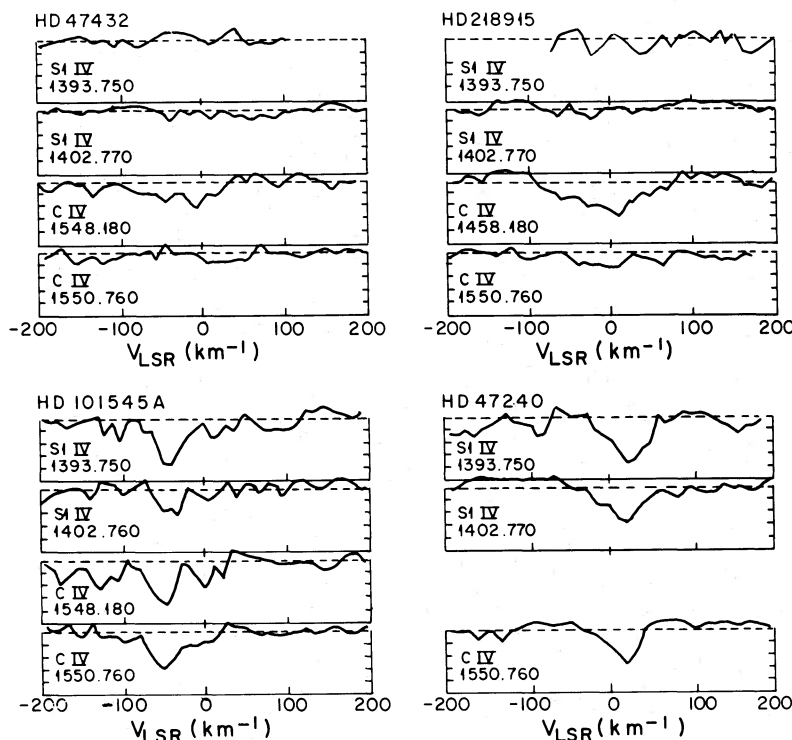


FIG. 9.—C IV profiles of the stars HD 218915 and HD 47432 are compared with more normal C IV and Si IV features. The relative broadness and shallowness of the components in these two stars should be noted.

shallow (Fig. 9) and that the velocity centroid of 218915 is very anomalous (Fig. 7) in not lying on the general $V_{\text{lsr}}-V_{\text{gr}}$ relationship. Both these results are expected if the gas arises in a uniformly distributed HIM.

We consider that these stars are the most like candidates showing the general distribution of the hot intercloud medium. If the line of sight to 218915 is representative, $n(\text{C IV}) \approx 2 \times 10^{-9} \text{ cm}^{-3}$ but a more extensive list of distant field stars is necessary to confirm the theory and refine this value.

VI. THE CARINA REGION

Only in one region (Carina) have we observed a high velocity component ($V_{\text{lsr}} \gtrsim 100 \text{ km s}^{-1}$) at the sensitivity of the survey. The negative wing is present in all the Carina stars (both Car OB1 and Car OB2) and appears to represent the negative velocity edge of a shell of gas of radius $\sim 100\text{--}200 \text{ pc}$ and expansion velocity $\sim 100 \text{ km s}^{-1}$. The shell of gas can be naturally understood in terms of ongoing energy injection by this active star forming region and appears very similar to the shell around the Ori OB1 and λ Ori associations (cf. Cowie, Songaila, and York 1979). We shall discuss this region in more detail in a subsequent paper (Cowie *et al.* 1981, in preparation).

VII. SUMMARY

While most of the C IV and Si IV absorption lines arise in H II regions from the target or from neighboring stars, some contribution to the C IV may also come from a generally distributed HIM with $n(\text{C IV}) \approx 2 \times 10^{-9} \text{ cm}^{-3}$. It is interesting to note that path lengths of several kiloparsecs are necessary for the uniformly distributed component to be observable and therefore it cannot account for the observations of C IV and Si IV in LMC stars (Savage and de Boer 1979) unless it has a large scale height. We have noted the existence of a uniform giant expanding region surrounding the Carina OB1 and OB2 associations.

This work was supported by grants NGL 31-001-007 and NAS 5-23576. The data were obtained as part of the IUE Guest Investigator Program, and we are most grateful to the staff and resident astronomers for their help in obtaining and reducing the data. We would also like to thank John Black for communicating his theoretical models of H II regions for comparison with our own, Ed Jenkins for numerous discussions and access to his notes on various aspects of this work, and John Raymond for a number of comments on the manuscript.

REFERENCES

- Aitken, R. G. 1932. *New General Catalogue of Double Stars* (Washington: Carnegie Institution).
- Aldrovandi, S. M. V., and Péquignot, D. 1973, *Astr. Ap.*, **25**, 137.
- Black, J. H., Dupree, A. K., Hartmann, L. W., and Raymond, J. C. 1980, *Ap. J.*, **239**, 502.
- Boggess, A., *et al.* 1978a, *Nature*, **275**, 372.
- Boggess, A., *et al.* 1978b, *Nature*, **275**, 377.
- Bruhwieler, F. C., Kondo, Y., and McCluskey, G. E. 1975, *Ap. J. (Letters)*, **229**, L39.
- Cowie, L. L., Hu, E., and York, D. G. 1981, preprint.
- Cowie, L. L., Jenkins, E. B., Songaila, A., and York, D. G. 1979, *Ap. J.*, **232**, 467.
- Cowie, L. L., and McKee, C. F. 1976, *Ap. J. (Letters)*, **209**, L105.
- Cowie, L. L., Songaila, A., and York, D. G. 1979, *Ap. J.*, **230**, 469.
- Dalgarno, A., and Butler, D. 1978, *Comments Atomic Molecular Phys.*, **7**, 129.
- Daltabuit, E., and Cox, D. P. 1972, *Ap. J.*, **177**, 855.
- Humphreys, R. M. 1970, *Astr. Ap. Suppl.*, **9**, 85.
- . 1975, *Astr. Ap. Suppl.*, **19**, 245.
- . 1978, *Ap. J. Suppl.*, **38**, 309.
- Innes, R. T. A. 1927, *Southern Double Star Catalogue* (Johannesburg: Union Observatory).
- Jenkins, E. B. 1980, preprint.
- Johnson, H. L. 1966, *Ann. Rev. Astr. Ap.*, **4**, 193.
- Kukarkin, B. V., *et al.* 1969, *General Catalogue of Variable Stars* (Moscow: Academy of Sciences of the USSR).
- Kurucz, R. 1979, *Ap. J. Suppl.*, **40**, 1.
- Raymond, J. C. 1976, Ph.D. thesis, University of Wisconsin.
- Sarazin, C. L. 1976, *Ap. J.*, **208**, 323.
- Savage, B. D., and de Boer, K. S. 1979, *Ap. J. (Letters)*, **230**, L77.
- Smith, L. J., Willis, A. J., and Wilson, R. 1980, *M.N.R.A.S.*, **191**, 339.
- Snow, T. P., and Morton, D. C. 1976, *Ap. J. Suppl.*, **32**, 429.
- Spitzer, L., and Jenkins, E. B. 1975, *Ann. Rev. Astr. Ap.*, **13**, 133.
- Watson, W. D. 1978, *Ann. Rev. Astr. Ap.*, **16**, 585.
- Weaver, R., McCray, R., Castor, J., Shapiro, P., and Moore, R. 1977, *Ap. J.*, **218**, 108.
- Weisheit, J. C. 1974, *Ap. J.*, **190**, 735.
- York, D. G. 1974, *Ap. J. (Letters)*, **193**, L127.
- . 1977, *Ap. J.*, **213**, 43.

LENNOX L. COWIE and DONALD G. YORK: Princeton University Observatory, Peyton Hall, Princeton, NJ 08544

WILLIAM TAYLOR: 64 Boston Avenue, Medford, MA 02155